International Scientific Journal
Environmental Science
http://environment.scientific-journal.com

Jet Impingement Cooling of a Rectangular Solid Heat Source Immersed in a Porous Layer

Nawaf H. Saeid and Azlina Diyanah Hamid
Mechanical Engineering Programme, Faculty of Engineering,
Institut Teknologi Brunei,
Jalan Tungku Link, Gadong BE 1410,
Brunei Darussalam
nawaf.saeid@itb.edu.bn; diyanah.hamid@itb.edu.bn

***Abstract*—In the present article the jet impingement cooling of a heated solid rectangular block immersed in a fluid saturated porous media is considered for numerical investigation. The jet direction is considered to be perpendicular from the top to the solid rectangular block which is heated from below. Therefore, the jet flow and the buoyancy driven flow are in opposite directions. For a fixed jet width, the governing parameters in the present Darcy flow problem are: Rayleigh number (Ra), Péclet number (Pe), solid to porous thermal conductivity ratio (K_r) and the dimensionless thickness (or height) of the solid wall (H). The results are presented in the mixed convection regime with wide ranges of the governing parameters with fixed jet width of 20% of the solid wall length. At low values of Pe (natural convection cases), it is found that the effect of Pe is negligible and the average Nusselt number (Nu) is increasing with the increase of either Rayleigh number or the thermal conductivity ratio or decreasing the thickness of the solid wall. At high values of Pe (forced convection cases), it is found that the effect of Ra is negligible and the Nu is increasing with increasing either Pe or the thermal conductivity ratio or decreasing the thickness of the solid wall. At moderated values of Pe (opposing mixed convection cases), it is observed that the values of average Nusselt number show minimum values for some values of Pe. The value of Pe at which minimum Nu occurs depends on Ra, thermal conductivity ratio and the thickness of the solid wall. At low values of either Ra or thermal conductivity ratio this case where Nu shows minimum value is not obvious. It is found that the thinner solid walls have higher values of the average Nusselt number with fixed other parameters. This due to the fact that thicker walls have higher thermal resistances to the heat dissipation from the isothermal surface with fixed other parameters.**

Keywords*—Jet impingment cooling, mixed convection, porous media

I. INTRODUCTION

The convection in porous media has been studied and analysed widely in recent years due to many applications in, for example, packed sphere beds, high performance insulation for buildings, electronic packages, chemical catalytic reactors, to name a few. Representative studies in this area may be found in the books by Nield and Bejan [1], Ingham and Pop [2], Vafai [3] and Kaviany [4].

It is noticed from the literature review that the jet impingement cooling through a highly conductive porous medium (metal foams) can be more effective as a heat sink than the simple jet impingement cooling. Prakash et al [5] and Fu and Huang [6] have considered the impinging jet studies in enclosures with and without a porous layer. A detailed flow visualization experiment has been carried out by Prakash et al. [5] to investigate the effect of a porous layer on flow patterns in an overlying turbulent flow without heat transfer. They studied the effect of the parameters such as the jet Reynolds number, the permeability of the porous foam, the thickness of the porous foam and the height of the overlying fluid layer. Fu and Huang [6] investigated numerically the effects of a laminar jet on the heat transfer performance of three different shape (rectangle, convex and concave) porous blocks mounted on a heated plate. They neglected the buoyancy effects and considered the forced convection mode only. Their results show that the heat transfer is mainly affected by a fluid flowing near the heated region. For a lower porous block, the three types of porous block enhance the heat transfer. However, for a higher porous block, the concave porous block only enhances heat transfer. Jeng and Tzeng [7] studied numerically the air jet impingement cooling of a porous metallic foam heat sink in the forced convection mode. They found the porous Aluminum foam heat sink could enhance the heat transfer from the heated horizontal source by impinging cooling. Their results show that the heat transfer performance of the Aluminum foam heat sink is 2 to 3 times larger than that without it. Saeid and Mohamad [8] studied the jet impingement cooling of a horizontal surface in a confined porous medium in the mixed convection regime. They conclude that at high values of Péclet number that increasing either Rayleigh number or jet width lead to increase the average Nusselt number. Narrowing the distance between the jet and the heated portion could increase the average Nusselt number as well. The non-Darcian effects on the mixed convection heat transfer from a metallic porous block subjected to confined slot jet is investigated numerically by Marafie et al [9]. Their results reveal that there is a substantial increase in heat transfer removal capability using a porous block with low porosity and high thermal conductivity.

Usually the heat source is bounded by a solid wall, for example, in the electronic cooling applications; the heat is generated in the electrical conductors which are surrounded by an electric insulation. Therefore the heat will be penetrating this wall of insulation to reach the heat sink for dissipation. In general the convection–conduction heat transfer through solid–porous layer can be found in many other engineering applications. Kimura et al [10] presented a review of conduction–convection conjugated natural convection from plates or bodies in a fluid saturated porous medium.

The literature shows many studies on the conjugate heat transfer in porous media for the food industry applications. Dirita et al [11] have analyzed numerically the air impingement cooling of cylindrical foods during the initial stage of cooling/chilling operations. They concluded that the local, time-dependent Nusselt number distribution in jet impingement cooling has been shown to be strongly dependent upon the conjugate effect, i.e. the heat transfer rate is altered by the conduction in the food. Numerical simulation of flow field and thermal transport processes for a turbulent jet impinging on the surface of a cylindrical object, were carried out by Nitin et al [12] at different jet velocities. Further experiments were carried out with real beef hotdogs to obtain center point temperature–time history during hot air impingement baking process. Rahman et al [13] and Bula et al [14] presented the results of numerical simulation of free jet of high Prandtl number fluid impinging on a solid substrate of finite thickness. They found that the average Nusselt number and the maximum temperature occurring in the solid varied significantly with impingement velocity (or Reynolds number), disk/plate thickness, and thermal conductivity of the disk/plate material. The transient conjugate heat transfer characterization of a free liquid jet impingement on a rotating solid disk is considered for numerical investigations by Rahman and Lallaye [15]. They found that the duration of the transient increased with disk thickness and decreased with Reynolds number and thermal conductivity ratio.

In the present study, the jet impingement cooling of a solid block heated from below immersed in a fluid saturated porous media is considered as shown in Fig. 1. The fluid saturated the porous media moving at a certain velocity, depends upon both the buoyancy effects and the velocity of the injected fluid. Such flows are of interest to engineers, for instance in cooling of electronic components, paper drying, food industry and agricultural products. The length of the heated solid wall is assumed to be two times the porous layer thickness, while the jet width is typically small comparing with the porous layer thickness, it is assumed to be (d = 0.2 L). The objective of the present study is to characterize the conjugate heat transfer where the jet impingement cooling is in the mixed convection regime with the limitation of the Darcy model.

II. Mathematical Model

The flow velocity in the porous layer is assumed to be low, therefore, the Darcy's law is assumed to hold and the thermal dispersion can be ignored. The Oberbeck–Boussinesq approximation is used for the fluid density–temperature relationship. The convective fluid and the porous media are in local thermal equilibrium. The properties of the fluid, the porous media and the solid wall are constants.

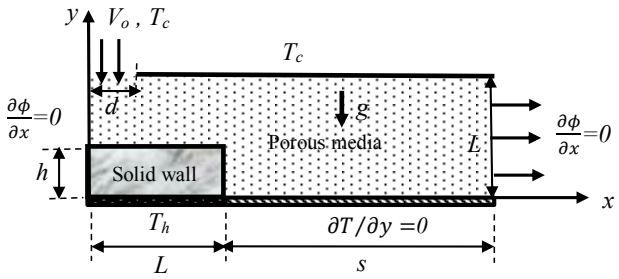

Fig. 1. Schematic diagram of the physical model and coordinate system.

With these assumptions, the continuity, Darcy and energy equation for steady, two-dimensional laminar flow in an isotropic and homogeneous porous medium are:

$$\frac{\partial u}{\partial x}+\frac{\partial v}{\partial y}=0 \tag{1}$$

$$u=-\frac{K}{\mu}\frac{\partial p}{\partial x} \tag{2a}$$

$$v=-\frac{K}{\mu}\left\{\frac{\partial p}{\partial y}+\rho_o g\left[1-\beta\left(T_p-T_o\right)\right]\right\} \tag{2b}$$

$$u\frac{\partial T_p}{\partial x}+v\frac{\partial T_p}{\partial y}=\alpha\left(\frac{\partial^2 T_p}{\partial x^2}+\frac{\partial^2 T_p}{\partial y^2}\right) \tag{3}$$

and the steady energy equation for the impermeable wall is:

$$\frac{\partial^2 T_w}{\partial x^2}+\frac{\partial^2 T_w}{\partial y^2}=0 \tag{4}$$

where the subscript p for porous layer and w for the wall. The subscript o for reference point and the Oberbeck–Boussinesq approximation $\rho\cong\rho_o\left[1-\beta\left(T-T_o\right)\right]$ is used in the body force term in equation (2b). By eliminating the pressure p from equations (2a) and (2b) a single momentum equation can be derived as:

$$\frac{\partial u}{\partial y}-\frac{\partial v}{\partial x}=-\frac{g\beta K}{\upsilon}\frac{\partial T_p}{\partial x} \tag{5}$$

where υ is the kinematic viscosity μ/ρ_o. The above equations can be written in terms of the stream function together with the following non-dimensional variables:

$$X=\frac{x}{L};\quad Y=\frac{y}{L};\quad D=\frac{d}{L};\quad H=\frac{h}{L}; \tag{6a}$$

$$\theta_p=\frac{T_p-T_c}{T_h-T_c};\ \theta_w=\frac{T_w-T_c}{T_h-T_c};\ U=\frac{u}{V_o}=\frac{\partial\Psi}{\partial Y};\ V=\frac{v}{V_o}=\frac{-\partial\Psi}{\partial X} \tag{6b}$$

The resulting non-dimensional forms of the governing equations (1)-(5) are:

$$\frac{\partial^2\Psi}{\partial X^2}+\frac{\partial^2\Psi}{\partial Y^2}=\frac{-Ra}{Pe}\frac{\partial\theta_p}{\partial X} \tag{7}$$

$$\frac{\partial\Psi}{\partial Y}\frac{\partial\theta_p}{\partial X}-\frac{\partial\Psi}{\partial X}\frac{\partial\theta_p}{\partial Y}=\frac{1}{Pe}\left(\frac{\partial^2\theta_p}{\partial X^2}+\frac{\partial^2\theta_p}{\partial Y^2}\right) \tag{8}$$

$$\frac{\partial^2\theta_w}{\partial X^2}+\frac{\partial^2\theta_w}{\partial Y^2}=0 \qquad (9)$$

where the Rayleigh number and Péclet numbers are defined respectively as:

$$Ra=\frac{g\beta K(T_h-T_c)L}{\upsilon\alpha};\qquad Pe=\frac{V_o L}{\alpha} \qquad (10)$$

The flow and heat transfer characteristics are symmetrical around *y*-axis as shown in Fig.1. Due to this symmetry, only one half is considered for the computational purpose and the boundary conditions are:

$$\Psi(0,Y)=\partial\theta_p(0,Y)/\partial X=\partial\theta_w(0,Y)/\partial X=0 \qquad (11a)$$

$$\partial\Psi(1+S,Y)/\partial X=\partial\theta_p(1+S,Y)/\partial X=0 \qquad (11b)$$

$$\Psi(X,0)=0\ ,\ \theta_w(X,0)=1 \text{ for } 0\le X\le 1$$
$$\text{and otherwise } \partial\theta_p(X,0)/\partial Y=0 \qquad (11c)$$

$$\theta_p(X,H)=0,\quad \Psi(X,H)=X \text{ , for } 0\le X\le D$$
$$\text{and otherwise } \Psi(X,H)=D \qquad (11d)$$

The solid-porous interface conditions are imposed as:

$$\theta_p(1,Y)=\theta_w(1,Y) \text{ and } \partial\theta_p(1,Y)/\partial X=K_r\,\partial\theta_w(1,Y)/\partial X \qquad (11e)$$

$$\theta_p(X,H)=\theta_w(X,H) \text{ and } \partial\theta_p(X,H)/\partial Y=K_r\,\partial\theta_w(X,H)/\partial Y \qquad (11f)$$

and

$$\Psi(X,Y)=0 \text{ for } 0\le X\le 1 \text{ and } 0\le Y\le H \qquad (11g)$$

where $K_r=k_w/k_p$ is the thermal conductivity ratio. The physical quantities of interest in this problem are the local Nusselt number and the average Nusselt number, defined respectively by:

$$Nu=\frac{-k_w(\partial T_w/\partial y)_{y=0}L}{k_p(T_h-T_c)}=-K_r\left(\frac{\partial\theta_w}{\partial Y}\right)_{Y=0};\qquad \overline{Nu}=\int_0^1 Nu.dX \qquad (12)$$

III. NUMERICAL SCHEME

Equations (7) - (9) subjected to the boundary conditions (11) are integrated numerically using the finite volume method described by Patankar [16] and Versteeg and Malalasekera [17]. The central differencing scheme is used for the diffusion terms of the energy equations (8) and (9) as well as for the momentum equation (7). The quadratic upwind differencing QUICK scheme [18] is used for the convection terms formulation of the energy equation (8). The linear extrapolation, known as mirror node approach, is used for the boundary conditions implementation.

The conditions at the interfaces (11e and 11f) have been implemented by approximating the temperature gradient in the solid wall region using the temperature at the interface and nearest two gird points as shown in Figure 2. Similar method is used for the porous medium and the temperature gradient is approximated by three-point forward difference scheme. The resultant wall–porous interface temperature can be derived as:

$$\theta_{wp}(i,Y)=\frac{9\theta_p(i+1,Y)-\theta_p(i+2,Y)+K_r[9\theta_w(i,Y)-\theta_w(i-1,Y)]}{8(1+K_r)} \qquad (13a)$$

$$\theta_{wp}(X,j)=\frac{9\theta_p(X,j+1)-\theta_p(X,j+2)+K_r[9\theta_w(X,j)-\theta_w(X,j-1)]}{8(1+K_r)} \qquad (13b)$$

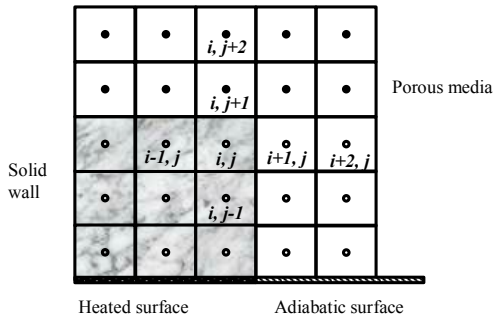

Fig. 2. Part of the mesh near the solid-porous interface

The resulting algebraic equations were solved by line-by-line using the Tri-Diagonal Matrix Algorithm iteration. The iteration process is terminated under the following condition:

$$\sum_{i,j}\left|\phi_{i,j}^{n}-\phi_{i,j}^{n-1}\right| \Big/ \sum_{i,j}\left|\phi_{i,j}^{n}\right| \le 10^{-5} \qquad (14)$$

where ϕ is the general dependent variable which can stands for either θ_p , θ_w or Ψ and *n* denotes the iteration step. To check the accuracy of the present numerical method and the results reported hereafter, energy balance has been employed since no experimental or numerical results were reported for this problem. The developed code is essentially a modified version of a code built and validated in previous work [19-21]. The energy balance requires that the heat lost by the lower hot portion must be equal to the heat transferred to the upper cold portion plus the heat being carried out by the fluid at the downstream end. This energy balance can be written in the present formulation as:

$$\int_0^L\left(-k_w\frac{\partial T_w}{\partial y}\right)_{y=0}dx=\int_0^{L+s}\left(-k_p\frac{\partial T_p}{\partial y}\right)_{y=L}dx+\int_0^L\left[\rho u C_p(T_p-T_c)\right]_{L+s}dy \qquad (15a)$$

In dimensionless form, it is reduced to:

$$\int_0^1\left(-K_r\frac{\partial\theta_w}{\partial Y}\right)_{Y=0}dX=\int_0^{1+S}\left(-\frac{\partial\theta_p}{\partial Y}\right)_{Y=1}dX+Pe\int_0^1\left(\frac{\partial\Psi}{\partial Y}\theta_p\right)_{1+S}dY \qquad (15b)$$

The solution domain is meshed using uniform cell size. The global energy balance has been checked for different mesh sizes and the results are presented in Table I. In Table I, % Error is used to show the percentage error in the energy balance and it means |(RHS – LHS)/RHS|*100, where RHS and LHS are the right hand side and the left hand side of equation (15) respectively. It is found from Table I that the mesh size (30×150) in the *Y* and *X* directions respectively with $S = 4$ gives satisfactory good results. The maximum error in the energy balance is found to be less than 2 % for the rage of $1 \le Pe \le 1000$ and $Ra = 100$. The global energy balance, equation (15) is used as additional convergence criterion to

stop the iterative solution. The difference in the values of the average Nusselt number using (150×30) is around 2%. Moreover, to check if S is large enough to ensure correct exit boundary condition (11b), the computational domain is doubled in X-direction, (i.e. $1+S = 10$) with mesh size (300×30). The results show differences around 1 % in the values of average Nusselt number due to duplication of the length of the computational domain and fixed other parameters. Hence $S = 4$ can be considered large enough to get acceptable accurate results and it is fixed with mesh size (150×30) to generate the results hereafter. .

TABLE I. Comparison of the results at different mesh sizes with Ra = 100, $H = 0.2$ and $K_r = 10$

	Mesh size (150×30) with $S = 4$		Mesh size (300×60) with $S = 4$		Mesh size (300×30) with $S = 9$	
Pe	*RHS* of Eq. (15)	% Error in Eq. (15)	*RHS* of Eq. (15)	% Error in Eq. (15)	*RHS* of Eq. (15)	% Error in Eq. (15)
1	4.443	1.74	4.440	1.59	4.443	1.74
10	4.287	2.23	4.275	1.91	4.284	2.35
25	3.406	1.26	3.369	1.58	3.400	1.48
50	3.948	1.25	3.819	0.16	3.949	1.24
100	5.011	0.47	4.958	0.10	4.942	0.91
1000	12.758	0. 08	12.618	0.27	12.745	0.19

IV. RESULTS AND DISCUSSION

Parametric study is carried out to investigate the heat and fluid flow characteristics. The governing parameters and their ranges considered in the present study are: thermal conductivity ratio parameter ($0.1 < K_r < 10$); thickness of the solid wall ($0.1 < H < 0.5$), Péclet number ($1 < Pe < 1000$) and Rayleigh number with the Darcy model limitations (Ra <= 100). As stated in the problem definition the jet inlet width D is fixed at $D = 0.2$ for all the simulation cases in the present study.

The variation of average Nusselt number with Péclet number for different values of Rayleigh number is shown in Fig. 3 with fixed values of $H = 0.2$ and $K_r = 10$. In the cases of natural convection domination, at low values of Péclet number, the effect of Pe is negligible on the heat transfer process. In this case (natural convection domination), the average Nusselt number can be increased by the increase in the Rayleigh number as shown in Fig. 3.

On contrast to that, at forced convection domination flow with high values of Pe, Fig. 3 shows that the effect of Rayleigh number is diminished and the variation of Nu with Pe for different values of Ra forming a single curve for Pe > 100. It can be observed from Fig. 3 that the values of Nu and therefore the heat transfer show minimum values for moderate values of Péclet number with high values of Rayleigh number. These values of Pe which result in minimizing the heat transfer are in-between the values of Pe for natural and forced convection domination, which is known as mixed convection. The present mixed convection mode is of opposing nature always since the jet flow is always opposing the buoyant flow.

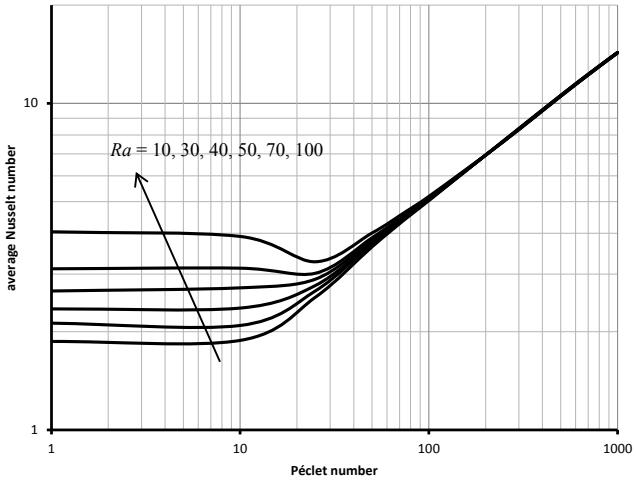

Fig. 3. Variation of average Nusselt number with Péclet number with $H = 0.2$ and $K_r = 10$.

The value of Pe at which minimum Nu occurs depends on Ra and at low values of Ra this case where Nu shows minimum value is not obvious. Moreover, numerical convergence difficulties encountered for the mixed convection cases, where maximum errors are found as shown in Table 1. This is due to the complex flow structure and an oscillatory convection is expected in some cases as discussed by Lai and Kulacki [22] and Saeid and Mohamad [8] for similar problem.

Fig. 4 depicted the details isotherms and streamlines for different values of Pe and fixed values of $H = 0.2$, $K_r = 10$ and Ra = 100, in which the mixed convection mode is clear as presented in Fig. 3 and Table 1. The dash lines in the streamlines represent the stagnant line with zero stream function. It can be observed from Fig.4 that two opposite rotating cells are formed for the cases of natural convection (Pe = 1 and Pe = 10) and mixed convection (Pe = 25) modes. For the natural convection cases, the streamlines of the jet inlet are comparatively weak and not obvious in these cases. For mixed convection mode (Pe = 25), the inflow from the jet modified the flow of the two cells and pushing them away from the heat source. In the forced convection domination, where *Pe* is high (Pe > 50), the two rotating cells are disappeared as shown in Fig. 4d, Fig. 4e and Fig. 3f. The isotherms show high negative gradients; especially in Fig. 3f, which leads to increase the heat transfer from the heated element.

The variation of the average Nusselt number with the Péclet number is shown in Fig. 5 for different values of K_r and fixed values of $H = 0.2$ and Ra =100. Fig. 5 shows that therefore the

average Nusselt number can be increased by increasing the thermal conductivity ratio parameter. In the cases of highly conductive wall ($K_r > 1$) the opposing mixed convection mode is clear and the heat transfer can be degraded, which leads minimum values of the average Nusselt number with moderated values of Pe as shown in Fig. 5. On the other hand of insulator walls (low conductive wall ($K_r < 1$) the variation of the average Nusselt number with Pe is almost a horizontal straight line as can be seen in Fig. 5.

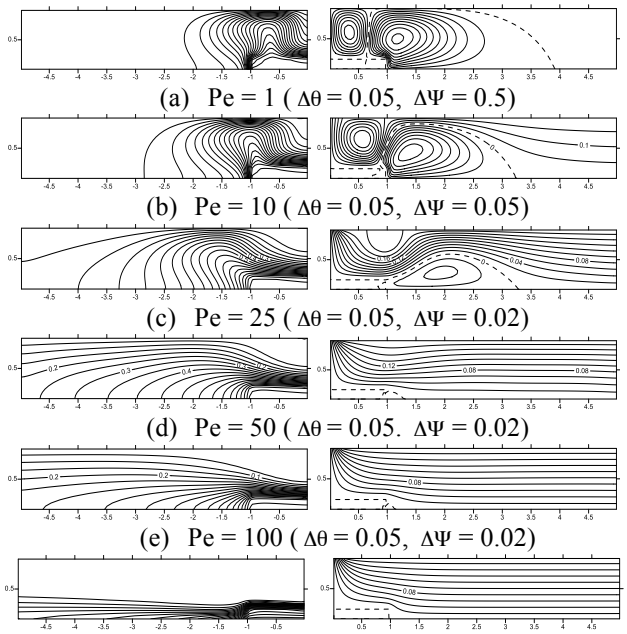

(a) Pe = 1 ($\Delta\theta = 0.05$, $\Delta\Psi = 0.5$)

(b) Pe = 10 ($\Delta\theta = 0.05$, $\Delta\Psi = 0.05$)

(c) Pe = 25 ($\Delta\theta = 0.05$, $\Delta\Psi = 0.02$)

(d) Pe = 50 ($\Delta\theta = 0.05$. $\Delta\Psi = 0.02$)

(e) Pe = 100 ($\Delta\theta = 0.05$, $\Delta\Psi = 0.02$)

(f) Pe = 1000 ($\Delta\theta = 0.05$, $\Delta\Psi = 0.02$)

Fig. 4. Isotherms (left), streamlines (right) with $H = 0.2$, $K_r = 10$ and Ra = 100.

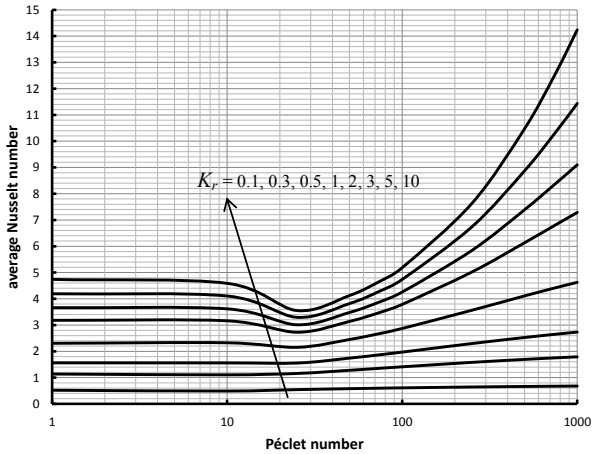

Fig. 5. Variation of average Nusselt number with Péclet number with $H = 0.2$ and Ra =100.

The effect of the solid wall thickness is studied by fixing the thermal conductivity ratio parameter ($K_r = 1$) and Rayleigh number (Ra =100). The variation of the average Nusselt number with Péclet number is shown in Fig. 6 for different values of the solid wall thickness. Obviously the solid wall placed on the top of the isothermal surface is increasing the thermal resistance and the thicker wall has the more resistance to the heat dissipation from the isothermal surface. The results presented in Fig. 6 prove this principle and the average Nusselt number for the thinner solid walls has higher values with fixed other parameters. Furthermore, the results in Fig.6 indicate that the values of average Nusselt number show minimum values for mixed convection conditions for thin solid walls only.

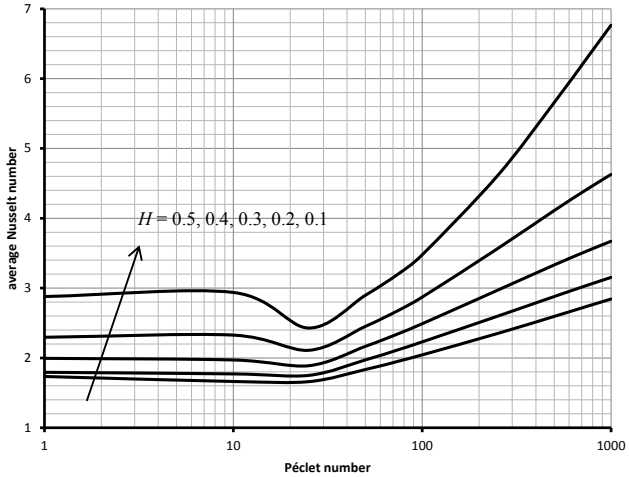

Fig. 6. Variation of average Nusselt number with Péclet number with $K_r = 1$ and Ra =100.

V. CONCLUSIONS

The jet impingement cooling of a heated solid rectangular block immersed in a fluid saturated porous media is investigated numerically. The external jet flow and the buoyancy driven flow are in opposite direction. The Darcy model is used in the mathematical model for the fluid flow through the porous media. The dimensionless governing parameters results from the mathematical model are the jet width (D), Rayleigh number (Ra), Péclet number (Pe), solid to porous thermal conductivity ratio (K_r) and the dimensionless thickness (or height) of the solid wall (H). After validation of the numerical method, the results are generated and presented in the mixed convection regime with wide ranges of the governing parameters with fixed jet width of 20% of the solid wall length. It is found, for natural convection domination cases (low values of Pe), the heat transfer can be enhanced by increasing either the Rayleigh number or the thermal conductivity ratio or decreasing the solid wall thickness. For the forced convention domination cases (high values of Pe) the results show that the values of average Nusselt number can be increased by increasing the Péclet number, thermal conductivity ratio and/or decreasing the solid wall thickness. The values of average Nusselt number show minimum values for some values of Péclet number for mixed convection conditions. The value of *Pe* at which minimum average Nusselt number occurs depends on *Ra* and at low values of *Ra* this case where average Nusselt number shows minimum value is not obvious. In the heat sink applications, the designers need to avoid the operation in these ranges of the governing parameters

in the opposing mixed convection in order to have effective cooling. It is found that the thinner solid walls with high thermal conductivity have higher values of the average Nusselt number with fixed other parameters. This due to the fact that thicker walls have higher thermal resistances to the heat dissipation from the isothermal surface with fixed other parameters. The high thermal conductivity solid walls can be used as heat spreaders by spreading the heat to larger surface area than the actual heat source and, therefore, enhance cooling.

ACKNOWLEDGMENT

The authors would like to acknowledge the financial support from the Institute Teknolgi Brunei and the Ministry of Education in Brunei Darussalam.

NOMENCLATURE

C_p	effective constant pressure specific heat
d	half of the width of the jet
g	gravitational acceleration
h	thickness (or height) of the solid layer
K	permeability of the porous medium
K_r	thermal conductivity ratio $(K_r = k_w/k_p)$
L	half of the heat source length
Nu	local Nusselt number
$\overline{Nu}$	average Nusselt number along the heat source
p	pressure
Pe	Péclet number
Ra	Rayleigh number for porous medium
s	distance from the heated portion to the end of the solution domain
T	temperature
u, v	velocity components
V_o	jet velocity
U,V	non-dimensional velocity components
x, y	Cartesian coordinates
X,Y	non-dimensional Cartesian coordinates

Greek symbols

α	effective thermal diffusivity
β	coefficient of thermal expansion
θ	non-dimensional temperature
μ	dynamic viscosity
υ	kinematic viscosity
ρ	density
ϕ	general dependent variable.
Ψ	non-dimensional stream function

REFERENCES

[1] D.A. Nield, A. Bejan, Convection in Porous Media, 4th ed., Springer, New York, 2013.

[2] D.B. Ingham, I. Pop (eds.): Transport Phenomena in Porous Media, vol. III. Elsevier, Oxford, 2005.

[3] K. Vafai (Ed.), Handbook of Porous Media, 2nd ed., Taylor & Francis, New York, 2005.

[4] M. Kaviany, Principles of Heat Transfer in Porous Media, 2nd ed., Springer, New York, 1995.

[5] M. Prakash, O.F. Turan, Y. Li, J. Mahoney, G.R. Thorpe, "Impinging round jet studies in a cylindrical enclosure with and without a porous layer: Part I—Flow visualizations and simulations", Chem. Eng. Sci., vol. 56, 2001, pp. 3855–3878.

[6] W.S. Fu, H.C. Huang, "Thermal performance of different shape porous blocks under an impinging jet", Int. J. Heat Mass Transfer, vol. 40, 1997, pp. 2261–2272.

[7] T.M. Jeng, S.C. Tzeng, "Numerical study of confined slot jet impinging on porous metallic foam heat sink", Int. J. Heat Mass Transfer, 48, 2005, pp. 4685–4694.

[8] N. H. Saeid, and A.A. Mohamad, "Jet impingement cooling of a horizontal surface in a confined porous medium: Mixed convection regime", Int. J. Heat Mass Transfer, vol. 49, 2006, pp. 3906–3913.

[9] A. Marafie, K. Khanafer, B. Al-Azmi and K. Vafai, "Non-Darcian effects on the mixed convection heat transfer in an metallic porous block with a confined slot jet", Numerical Heat Transfer, Part A, vol. 55, 2008, pp. 665-685.

[10] S. Kimura, T. Kiwata, A. Okajima, I. Pop, "Conjugate natural convection in porous media", Advances in Water Resources, vol. 20, 1997, pp. 111–126.

[11] C. Dirita, M. Valeria De Bonis and G. Ruocco, "Analysis of food cooling by jet impingement, including inherent conduction", Journal of Food Engineering, vol. 81, 2007, pp. 12–20.

[12] N. Nitin, R.P. Gadiraju, and M.V. Karwe, "Conjugate heat transfer associated with a turbulent hot air jet impinging on a cylindrical object", Journal of Food Process Engineering, vol. 29, 2006, pp. 386-388.

[13] M.M. Rahman, A.B. Bula and J.E. Leland, "Conjugate heat transfer during free jet impingement of a high Prandtl number fluid", Numerical Heat Transfer, Part B: Fundamentals, vol. 36, 1999, pp. 139-162.

[14] A.B. Bula, M.M. Rahma, and J.E. Leland, "Numerical modeling of conjugate heat transfer during impingement of free liquid jet issuing from a slot nozzle, Numerical Heat Transfer", Part A: Applications, vol. 38, 2000, pp. 45-66.

[15] M.M. Rahman and J.C. Lallaye, "Transient conjugate heat transfer during free liquid jet impingement on a rotating solid disk, Numerical Heat Transfer", Part A: Applications, vol. 55, 2009, pp. 229-251.

[16] S.V. Patankar, Numerical Heat Transfer and Fluid Flow, in: W.J. Minkowycz, E.M. Sparrow (Eds.), Computational Methods in Mechanics and Thermal Sciences, McGraw-Hill, New York, 1980.

[17] H.K. Versteeg, W. Malalasekera, An Introduction to Computational Fluid Dynamics, the Finite Volume Method, Longman, England, 1995.

[18] T. Hayase, J.A.C. Humphrey, R. Greif, "A consistently formulated QUICK scheme for fast and stable convergence using finite-volume iterative calculation procedures", J. Comput. Phys., vol. 98, 1992, pp. 108–118.

[19] N. H. Saeid and I. Pop, "Mixed convection from two thermal sources in a vertical porous layer", Int. J. Heat Mass Transfer, vol. 48, 2005, pp. 4150-4160.

[20] N.H. Saeid, "Conjugate natural convection in a porous enclosure: effect of conduction in one of the vertical walls", Int. J Therm. Sci., vol. 46, 2007, pp. 531–539.

[21] N.H. Saeid, "Conjugate natural convection in a porous enclosure sandwiched by finite walls under thermal non-equilibrium conditions". J. Porous Media, vol. 11, 2008, pp. 259–275.

[22] F.C. Lai and F.A. Kulacki, "Oscillatory mixed convection in horizontal porous layers heated from below", Int. J. Heat Mass Transfer, vol. 34, 1991, pp. 887-890.